



Coexisting attractors and circuit implementation of a new 4D chaotic system with two equilibria



Qiang Lai^a, Tsafack Nestor^b, Jacques Kengne^c, Xiao-Wen Zhao^{d,*}

^a School of Electrical and Automation Engineering, East China Jiaotong University, Nanchang, 330013, China

^b Laboratory of Electronics and Signal Processing, Department of Physics, University of Dschang, Dschang, P.O. Box 67, Cameroon

^c Laboratory of Automation and Applied Computer, Department of Electrical Engineering, University of Dschang, Bandjoun, P. O. Box 134, Cameroon

^d School of Mathematics, Hefei University of Technology, Hefei, 230009, China

ARTICLE INFO

Article history:

Received 2 August 2017

Revised 31 October 2017

Accepted 21 December 2017

Keywords:

New 4D chaotic system

Coexisting attractors

Circuit implementation

Bifurcation diagram

Lyapunov spectrum

ABSTRACT

This letter proposes a new 4D autonomous chaotic system characterized by the abundant coexisting attractors and a simple mathematical description. The new system which is constructed from the Sprott B system is dissipative, symmetric, chaotic and has two unstable equilibria. For a given set of parameters, butterfly attractors are emerged from the system. These butterfly attractors will be broken into a pair of symmetric strange attractors with the variation of the parameters. A variety of coexisting attractors are spotted in the system including six periodic attractors, four periodic attractors with two chaotic attractors, two periodic attractors with three chaotic attractors, two periodic attractors with two chaotic attractors, four periodic attractors, etc. Finally, the system is established via an electronic circuit which can physically confirm the complex dynamics of the system.

© 2017 Elsevier Ltd. All rights reserved.

1. Introduction

The multistability characterized by multiple coexisting attractors in a system is an exceedingly interesting phenomenon which has aroused increasing attention in scientific community. Especially in recent years, the study of the coexisting attractors in chaotic systems has become a focus for many researchers. It is really amazing that an autonomous differential system not only generates chaotic attractors but also generates several independent attractors depending solely on the system's initial states. A typical example is the well-known Lorenz system which yields a symmetric pair of strange attractors with the breaking of butterfly attractor [1]. The Newton–Leipnik system that describes the rigid body motion is also a very representative system with two concurrent butterfly attractors [2]. Actually, through in-depth study, many of the existing 3D chaotic systems have been found to exhibit coexisting attractors for special parameter values and initial values, such as Chua system, Sprott system, Rabinovich–Fabrikant system, Jerk system, etc [3–8]. On the basis of 3D chaotic systems, 4D and 5D chaotic systems with multiple strange attractors are constructed by using linear and nonlinear feedback control [9–12]. Also some no-equilibria chaotic systems with multiple hidden attractors were numerically and experimentally presented [13–15]. The memristor-

based circuit systems which can be described by smooth nonlinear differential equations are capable of generating a wealth of coexisting attractors [16–18]. Interestingly, Li et al. put forward a method of conditional symmetry for constructing chaotic system with coexisting attractors [19]. Lai et al. generated multiple butterfly attractors from the Sprott B system by applying a polynomial function method [20]. The coexisting attractors is ubiquitous in many natural systems and usually plays an important impact on the performance of the systems [21–23]. The system can switch between its multiple steady states for adapting to a changeable external environment. The study of chaos seems to have reached its maturity today as so many literatures addressed on it [24–30]. However, the coexisting attractors, as a new research direction in chaos theory, are still in its infancy. This letter focuses on the investigation of the coexisting attractors in a new 4D autonomous chaotic system which is generated from the 3D Sprott B system. Both simulation and circuit analysis determine the coexistence of multiple attractors in the system. It shows that the system is rich in different types of coexisting attractors for different parameter sets and initial values, including six periodic attractors, four periodic attractors with two chaotic attractors, two periodic attractors with three chaotic attractors, two periodic attractors with two chaotic attractors, four periodic attractors, etc.

* Corresponding author.

E-mail address: zhaoxiaowen@hfut.edu.cn (X.-W. Zhao).

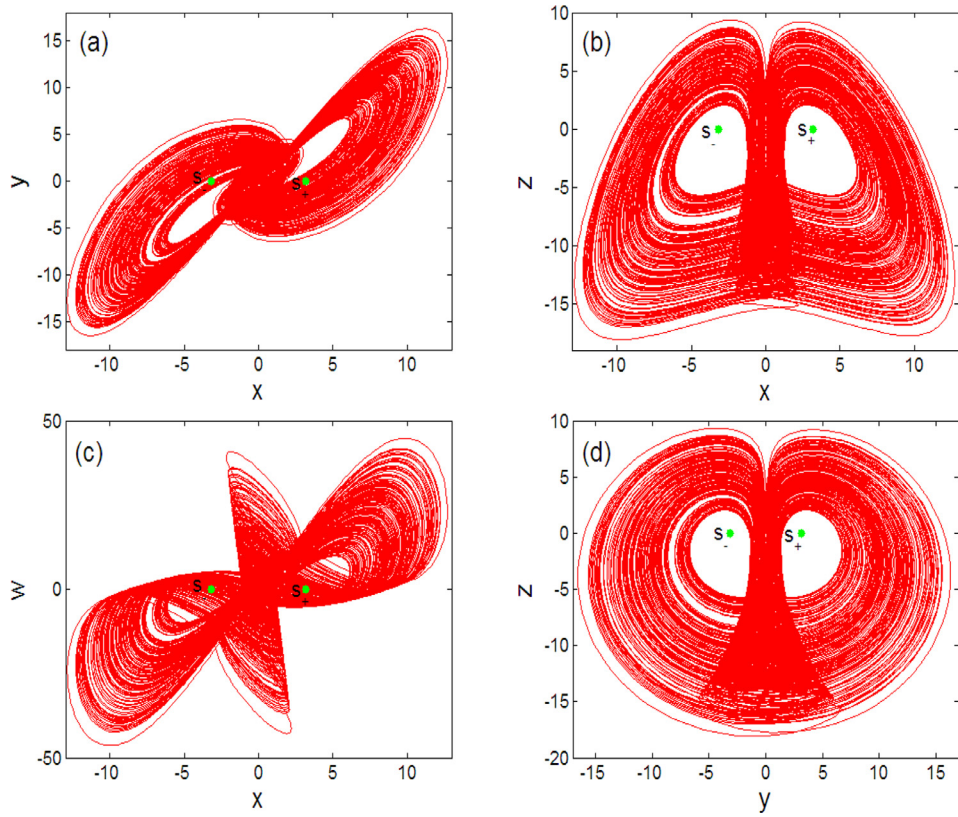


Fig. 1. A butterfly attractor of system (1) with $a = 10, b = 10, c = 3$: (a) $x - y$; (b) $x - z$; (c) $x - w$; (d) $y - z$.

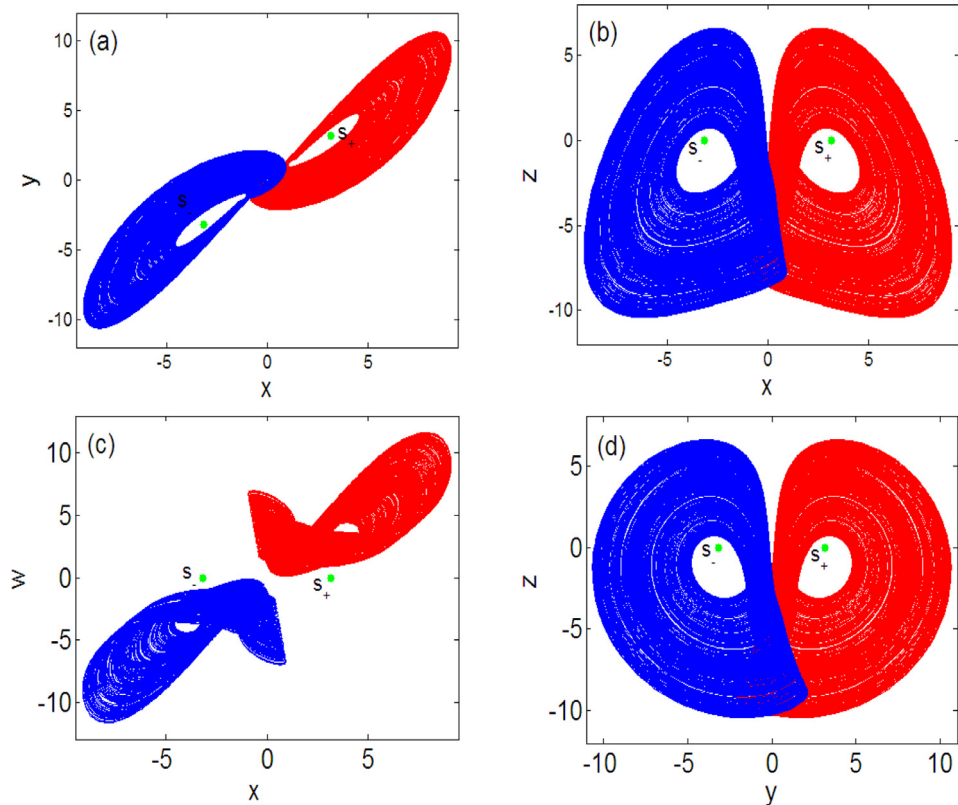


Fig. 2. A pair of strange attractors of system (1) with $a = 10, b = 10, c = 1$: (a) $x - y$; (b) $x - z$; (c) $x - w$; (d) $y - z$.

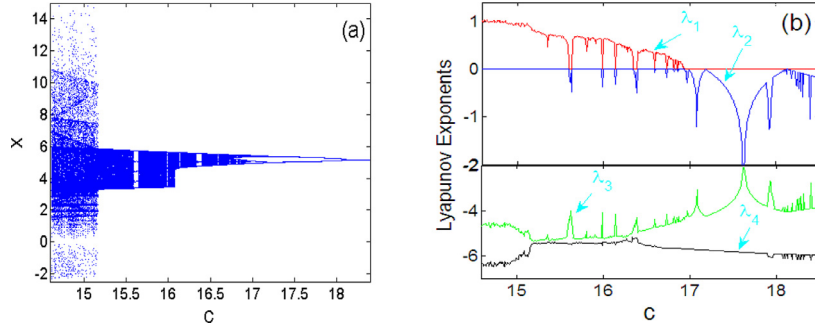


Fig. 3. The bifurcation diagram and Lyapunov spectrum of system (1) for $a = b = 10$ as c varies. It can be noticed that the system (1) experiences the reverse period doubling bifurcation route to chaos.

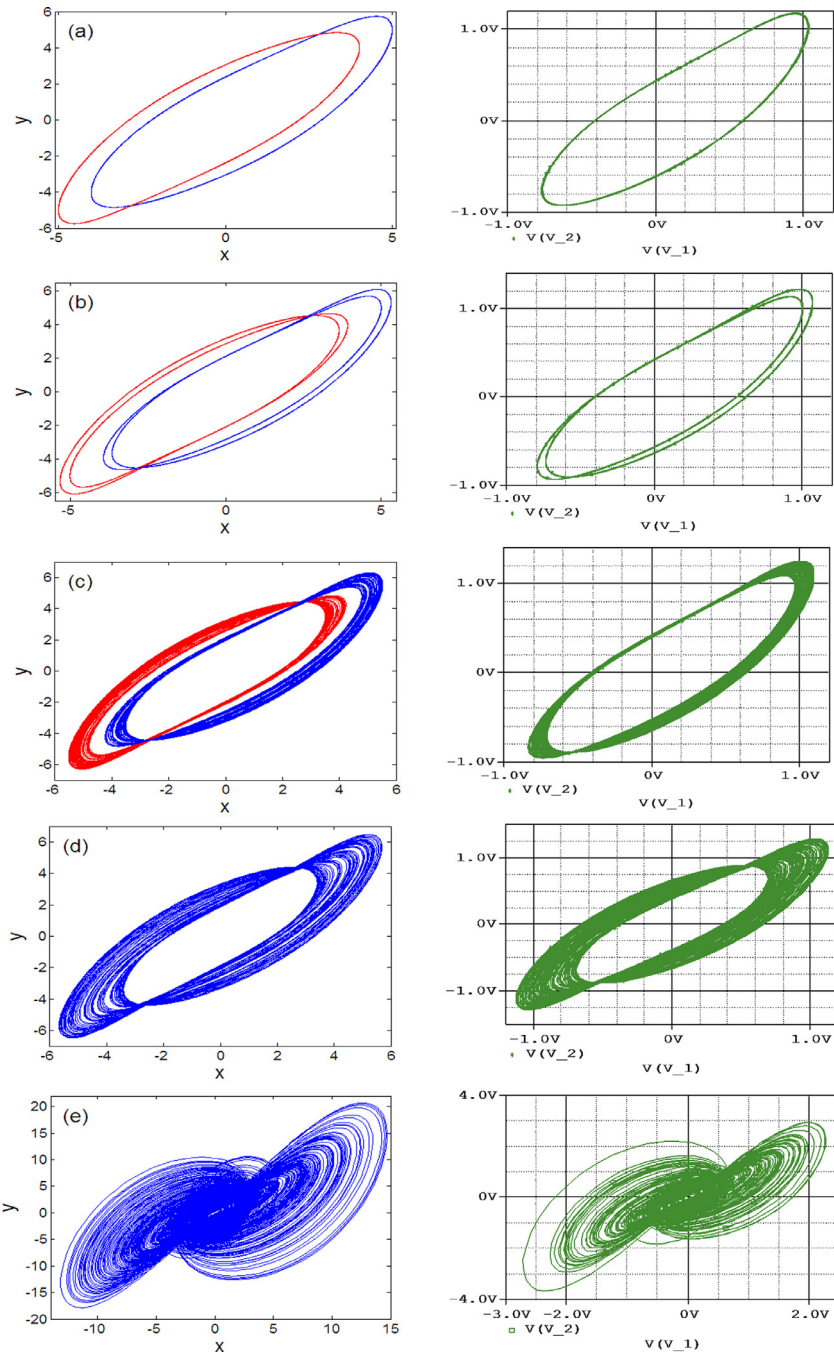


Fig. 4. Numerical phase space trajectories (left) and Pspice based simulation results (right) showing the classical period doubling routes to chaos in system (1).

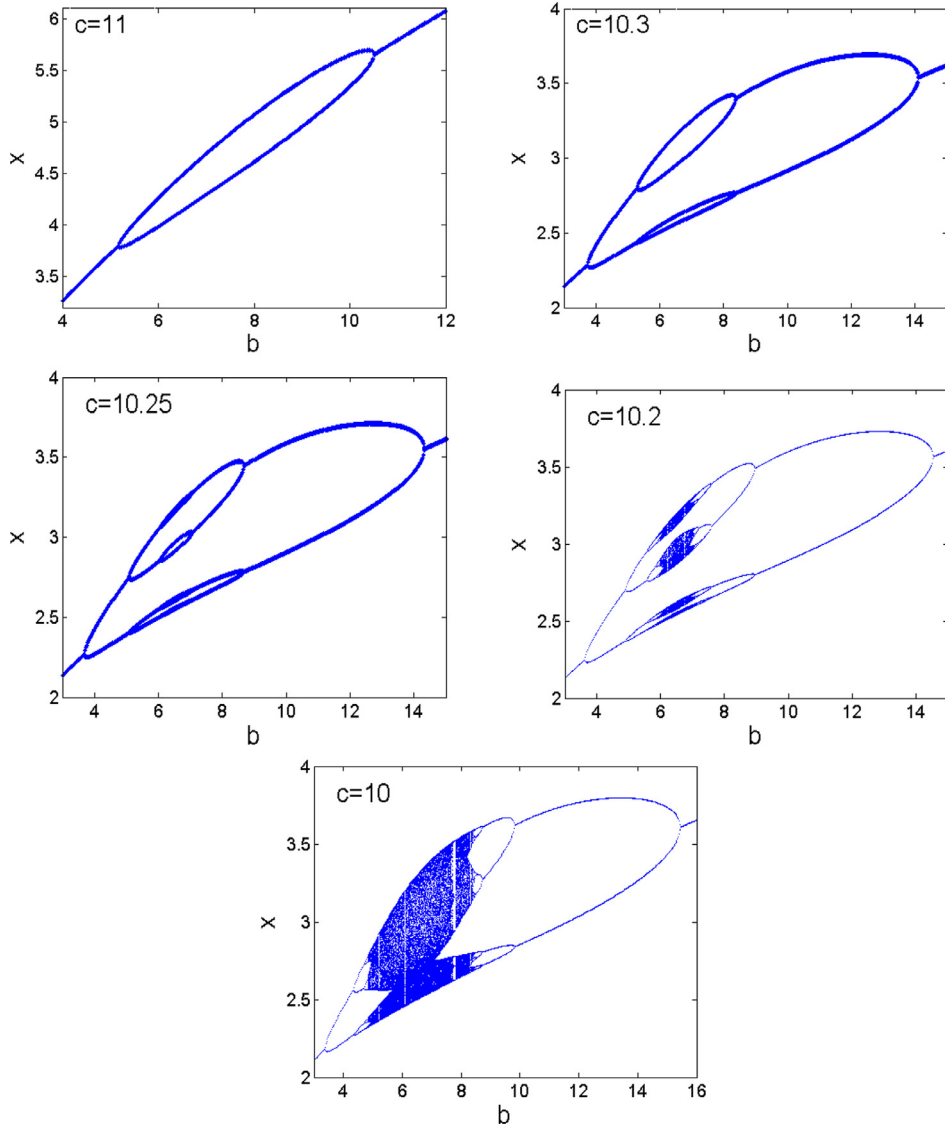


Fig. 5. The bifurcation diagrams showing local maxima of the coordinate x of the attractor in Poincaré cross section in terms of the control parameter for remerging Feigenbaum tree (bubbling).

2. System description

The mathematical model of the new 4D chaotic system presented in this paper can be expressed by the following autonomous differential equations:

$$\begin{cases} \dot{x} = a(y - x) \\ \dot{y} = xz + w \\ \dot{z} = b - xy \\ \dot{w} = cyz \end{cases} \quad (1)$$

where x, y, z, w are state variables, a, b, c are positive real numbers. The system (1) is constructed from the 3D Sprott B system [24] by introducing an additional variable w with nonlinear derivative function $\dot{w} = cyz$. To our best knowledge, there is no existing literature that has reported this system before with such complex dynamics. The uniqueness of the system (1) is that it has extremely unique dynamical behavior, especially various types of coexisting attractors.

The system (1) is dissipative since its divergence ($\nabla V = -a$) is negative. It indicates that system (1) will eventually form an attractor as the time approaches infinity. Under the coordinate transformation $(x, y, z, w) \rightarrow (-x, -y, z, -w)$, system (1) will re-

main unchanged. It means that system (1) is symmetric with respect to x -axis, y -axis, w -axis. This will be partially reflected in the equilibria and attractors of system (1). By assuming that $\dot{x} = \dot{y} = \dot{z} = \dot{w} = 0$, the equilibria of system (1) can be calculated as $S_{\pm}(\pm\sqrt{b}, \pm\sqrt{b}, 0, 0)$. Linearizing the system (1) at S_{\pm} , we can easily deduce that the eigenvalues of the corresponding Jacobian matrix should meet the following equation

$$\lambda^4 + a\lambda^3 + b\lambda^2 + (2a + c)b\lambda + 2abc = 0 \quad (2)$$

It can be easily verified that S_{\pm} are unstable with $a > 0, b > 0, c > 0$ via the classic Routh–Hurwitz stability criterion.

3. Butterfly chaotic attractor

For the parameters $a = 10, b = 10, c = 3$ and initial value $(1, 1, 0, 0)$, a butterfly attractor can be numerically observed in system (1), as its projections on the various planes are shown in Fig. 1, where the green points represent the equilibria $S_{\pm}(\pm\sqrt{10}, \pm\sqrt{10}, 0, 0)$. The Lyapunov exponents of the system (1) can be calculated as $l_1 = 0.4980, l_2 = 0, l_3 = -2.7728, l_4 = -7.7252$. It follows that the corresponding Lyapunov dimension is $D_L = 3 - l_1/(l_3 + l_4) = 3.0474$. Thus the attractor is a strange attractor with fractal dimension.

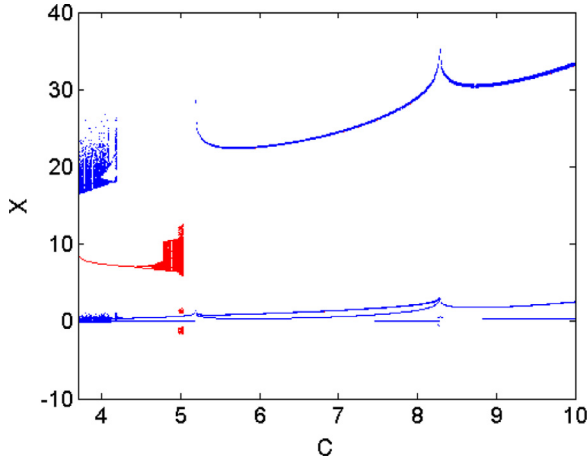


Fig. 6. The bifurcation diagrams for illustrating a maximum of four coexisting attractors in the phase space with $a = 50, b = 20$.

Reset the parameter $c = 1$ and keep the parameters a, b unchanged, then two independent attractors are yielded in system (1) from the initial values $(\pm 1, \pm 1, 0, 0)$, as shown in Fig. 2. It can be verified that the attractors are chaotic as they have the same positive maximum Lyapunov exponent $l_1 = 0.1590 > 0$ and fractal Lyapunov dimension $D_l = 3.0157$. Accordingly, the butterfly attractor in Fig. 1 is broken into two strange attractors with smaller maximum Lyapunov exponent in Fig. 2. The two strange attractors have very similar characteristics and coordinate symmetry.

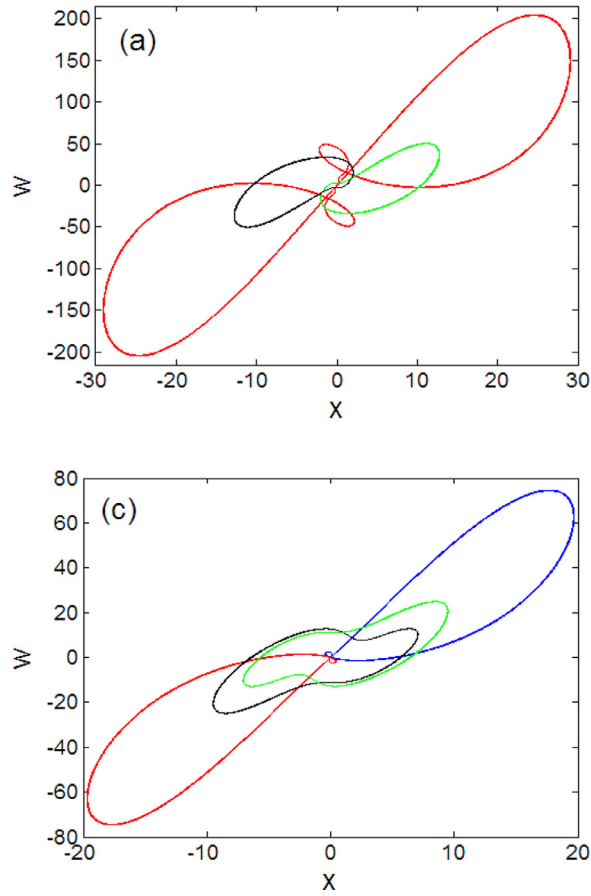


Fig. 7. Multiple coexisting attractors for $a = 50, b = 20$: (a) $c = 8$ (three limit cycles); (b) $c = 4.872$ (two limit cycles and a chaotic attractor); (c) $c = 4.418$ (four limit cycles); (d) $c = 4.733$ (two limit cycles and two chaotic attractors).

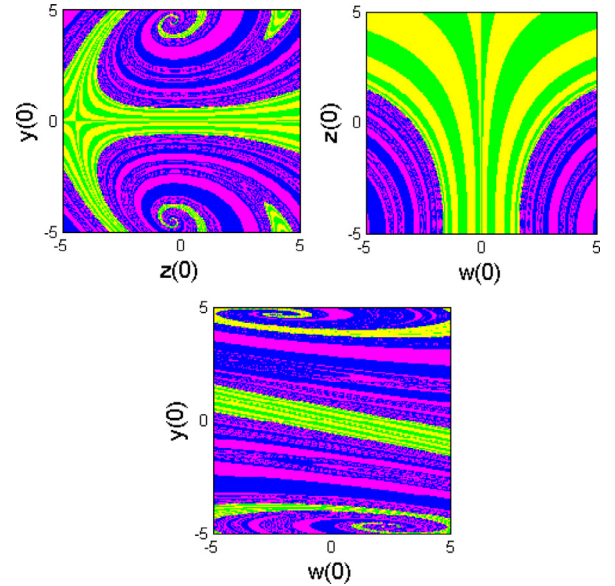
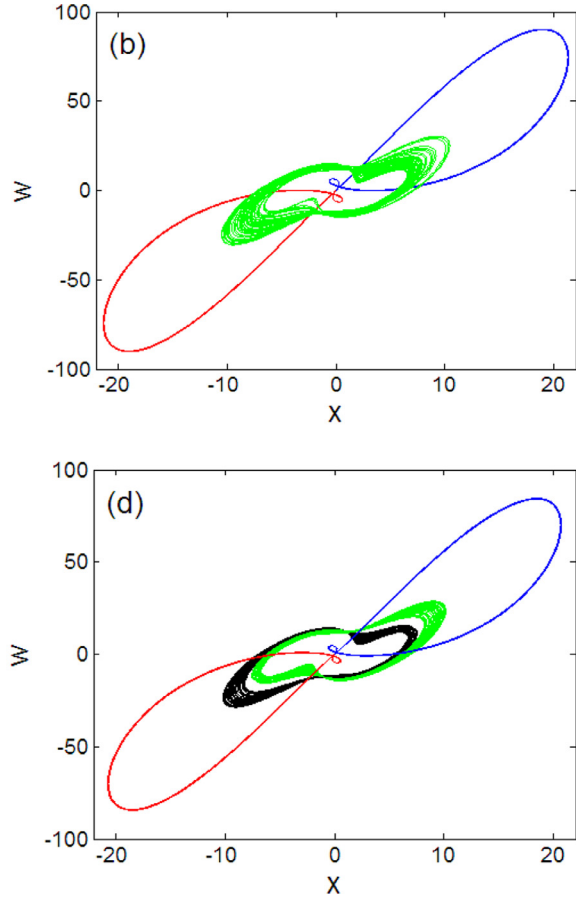


Fig. 8. Cross sections of the basin of attraction for $x(0) = 0, y(0) = 0, z(0) = 0$ and $w(0) = 0$, respectively, corresponding to the asymmetric pair of periodic attractors (green and yellow) and the pair of chaotic attractors (blue and magenta) obtained for $a = 50, b = 20, c = 4.733$. (For interpretation of the references to colour in this figure legend, the reader is referred to the web version of this article.)

4. Routes to chaos and antimonotonicity

To investigate the sensitivity of the system (1) with respect to a single control parameter, we fix $a = b = 10$ and vary c in the range



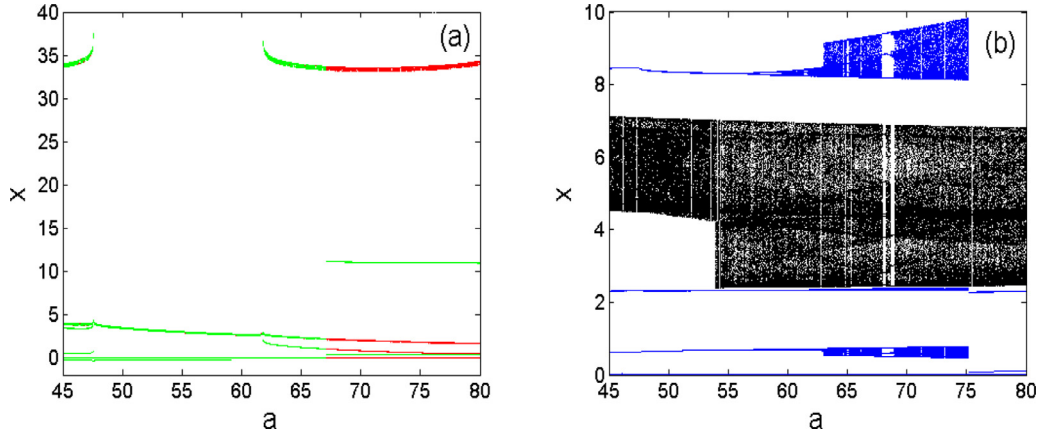


Fig. 9. The bifurcation diagrams for illustrating a maximum of six coexisting attractors in the phase space with $b = 8, c = 10$.

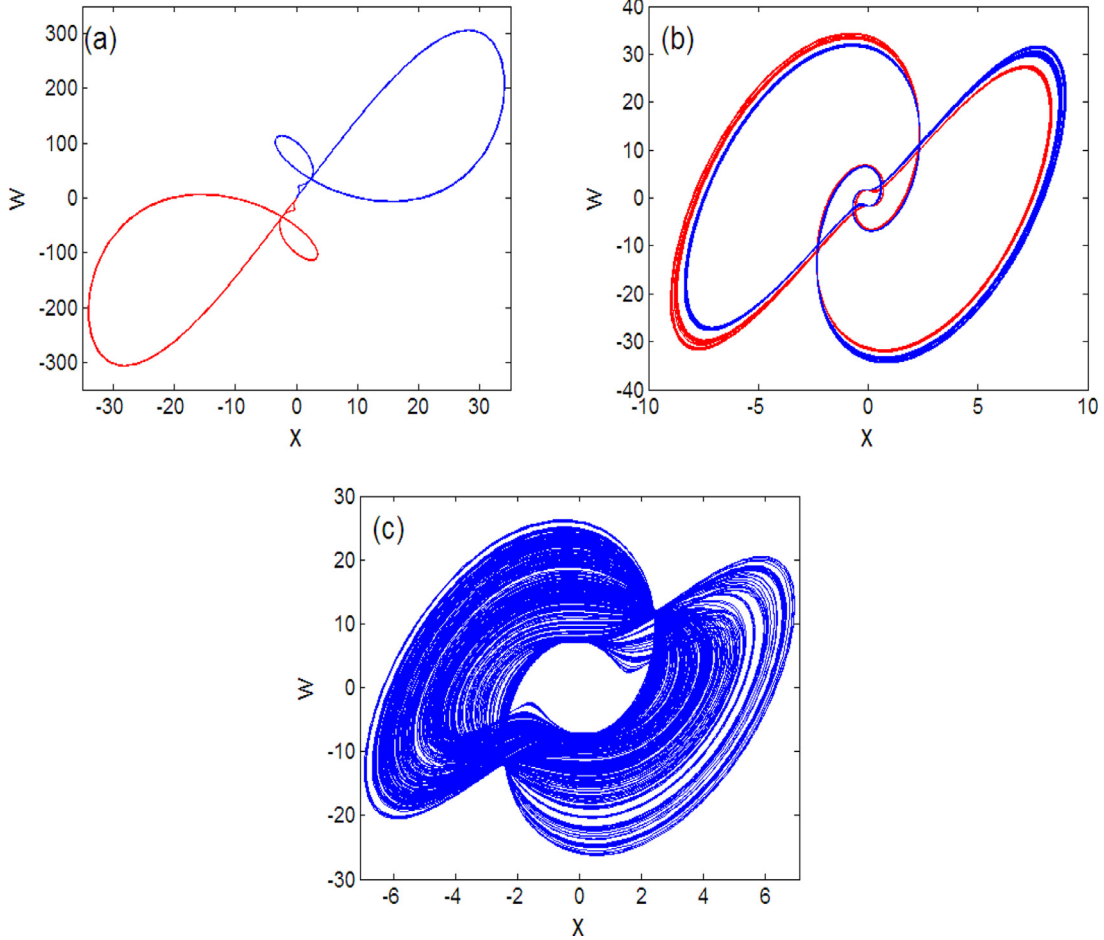


Fig. 10. Five coexisting attractors for $a = 60, b = 8, c = 10$: (a) two limit cycles with initial values $(0, \pm 2.7, 0, 0)$; (b) two chaotic attractor for initial values $(0, \pm 0.9, 0, 0)$; (c) a symmetric chaotic attractor for initial value $(1, 0, 0, 0)$.

$14.5 < c < 18.5$. It is clear from the bifurcation diagram of Fig. 3 that the system (1) experiences the well known reverse period doubling route to chaos with the initial values $(\pm 1, \pm 1, 0, 0)$. For $c = 18.5$, system (1) has a period-1 attractor. For $c = 17.5$, system (1) has a period-2 attractor. Asymmetric attractor of system (1) is obtained for $c = 16.5$. Symmetric attractors of system (1) are observed at $c = 15.81$ and $c = 15$. The various attractors (numerical simulations) illustrating the above described routes to chaos are depicted in Fig. 4-left.

As the route to chaos is the classical period doubling bifurcation, it is obvious that the system (1) experiences the antimonotonicity. This is the creation and annihilation of periodic orbits. This dynamics can be obtained by setting $a = 5$ and by varying parameter b for some discrete values of parameter c : period-2 bubble is obtained for $c = 11$, period-4 bubble is observed for $c = 10.3$, period-8 bubble is obtained for $c = 10.25$ and full Feigenbaum remerging tree is observed for $c = 10$ (Fig. 5).

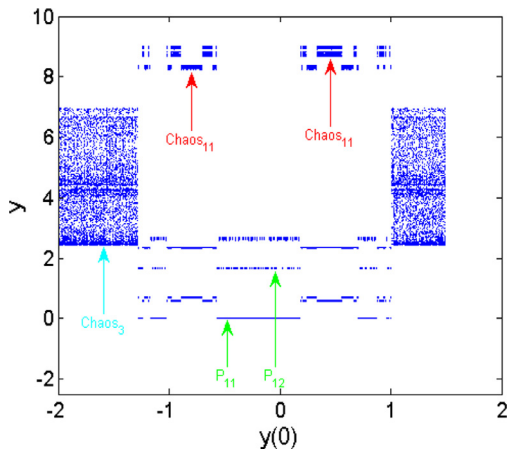


Fig. 11. Bifurcation diagram showing local maxima of the coordinate y versus initial value $y(0)$ plotted in the range $[-2, 1.5]$. The system parameters being fixed to $a = 60$, $b = 8$, $c = 10$ and the rest of initial values fixed as $x(0) = z(0) = w(0) = 1$.

5. Multiple coexisting attractors

The coexistence of multiple attractors in the system (1) can be determined by plotting the bifurcation diagrams. Setting $a = 50$, $b = 20$, then the bifurcation diagrams of system (1) can be plotted by forward and backward continuation of parameter c as shown in Fig. 6, where the red and blue color branches respectively generate from initial values $(1, 1, 0, 0)$, $(1, 0, 0, 0)$. The bifurcation diagrams of system (1) with initial values $(-1, -1, 0, 0)$, $(-1, 0, 0, 0)$ are also available owing to the symmetry of system

(1). From the Fig. 6, we can notice an hysteretic behavior leading to several windows in which attractors coexist in the phase space. The coexisting attractors can be visually presented by plotting the corresponding phase portraits, as shown Fig. 7. Three periodic attractors coexist at $c = 8$ with the initial values $(1, 0, 0, 0)$ and $(\pm 1, \pm 1, 0, 0)$. Two periodic attractors and a symmetric chaotic attractor coexist at $c = 4.872$ with the initial values $(\pm 1, 0, 0, 0)$ and $(1, 1, 0, 0)$. Four periodic attractors coexist at $c = 4.418$ with the initial values $(\pm 1, 0, 0, 0)$ and $(\pm 1, \pm 1, 0, 0)$. Two periodic attractors and two chaotic attractors coexist at $c = 4.733$ with the initial values $(\pm 1, 0, 0, 0)$ and $(\pm 1, \pm 1, 0, 0)$. The basin of attraction of system (1) with parameters $a = 50$, $b = 20$, $c = 4.733$ is also plotted for illustrating the coexistence of two periodic attractors and two chaotic attractors, as shown in Fig. 8.

For $b = 8$, $c = 10$, another interesting hysteretic dynamics is observed in system (1) by plotting the bifurcation diagrams (see Fig. 9) and taking a as the control parameter. These diagrams confirm the coexistence of five different attractors for $a = 60$ (see Fig. 10) where we have: (a) Two periodic limit cycles with initial values $(0, \pm 2.7, 0, 0)$; (b) two chaotic attractor with initial values $(0, \pm 0.9, 0, 0)$; (c) a symmetric chaotic attractor with initial value $(1, 0, 0, 0)$. The coexistence of five attractors in system (1) with $a = 60$, $b = 8$, $c = 10$ can also be determined by plotting the bifurcation diagram with initial values $x(0) = z(0) = w(0) = 1$ and $y(0) \in [-2, 1.5]$, as shown in Fig. 11. It illustrates the types of chaotic attractors and periodic attractors coexist in system (1) for different range of initial values. Six periodic attractors coexist for $a = 51.89$ and initial values $(\pm 1, 0, 0, 0)$, $(0, \pm 0.9, 0, 0)$, $(\pm 1, \pm 1, 0, 0)$ are shown in Fig. 12. Six attractors coexist for $a = 50$ and initial values $(\pm 1, 0, 0, 0)$, $(1, 1, 1, 1)$, $(1, 1, 1, -2)$, $(\pm 1, \pm 1, 0, 0)$ are shown in Fig. 13. We also can verify the coexistence of six attractors of the system (1) with parameters $a = 50$, $b = 8$, $c = 10$ by

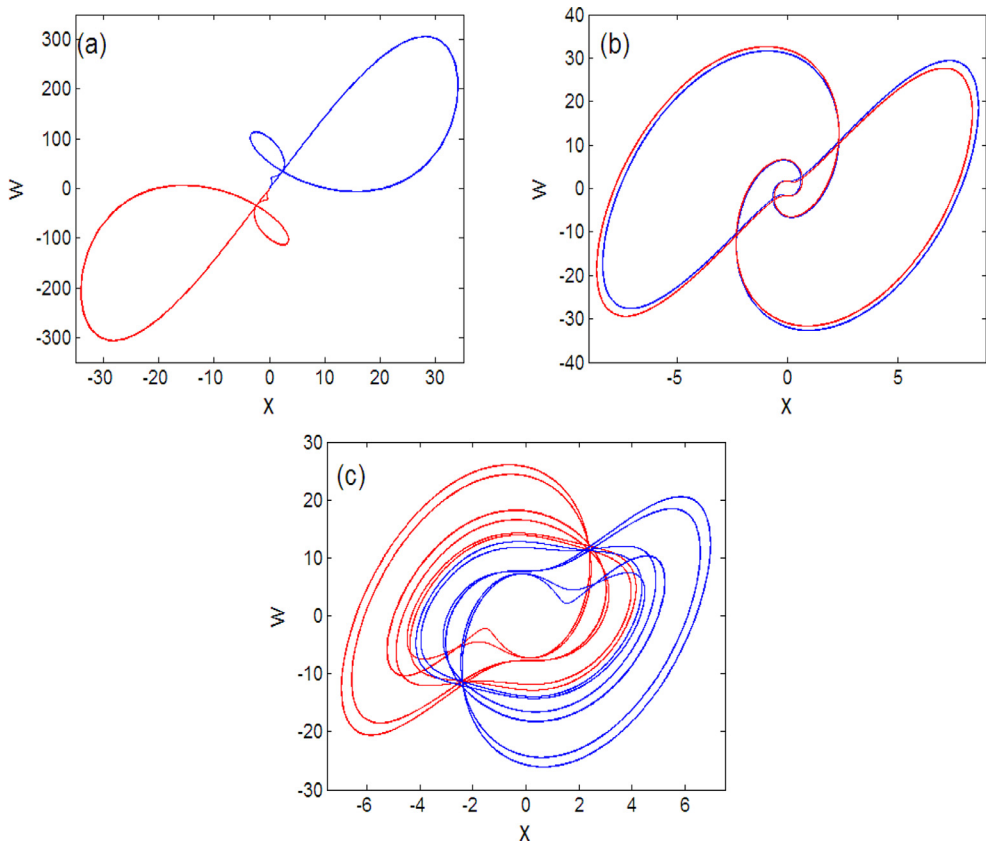


Fig. 12. Six coexisting periodic attractors for $a = 51.89$, $b = 8$, $c = 10$ and initial values $(\pm 1, 0, 0, 0)$, $(0, \pm 0.9, 0, 0)$, $(\pm 1, \pm 1, 0, 0)$.

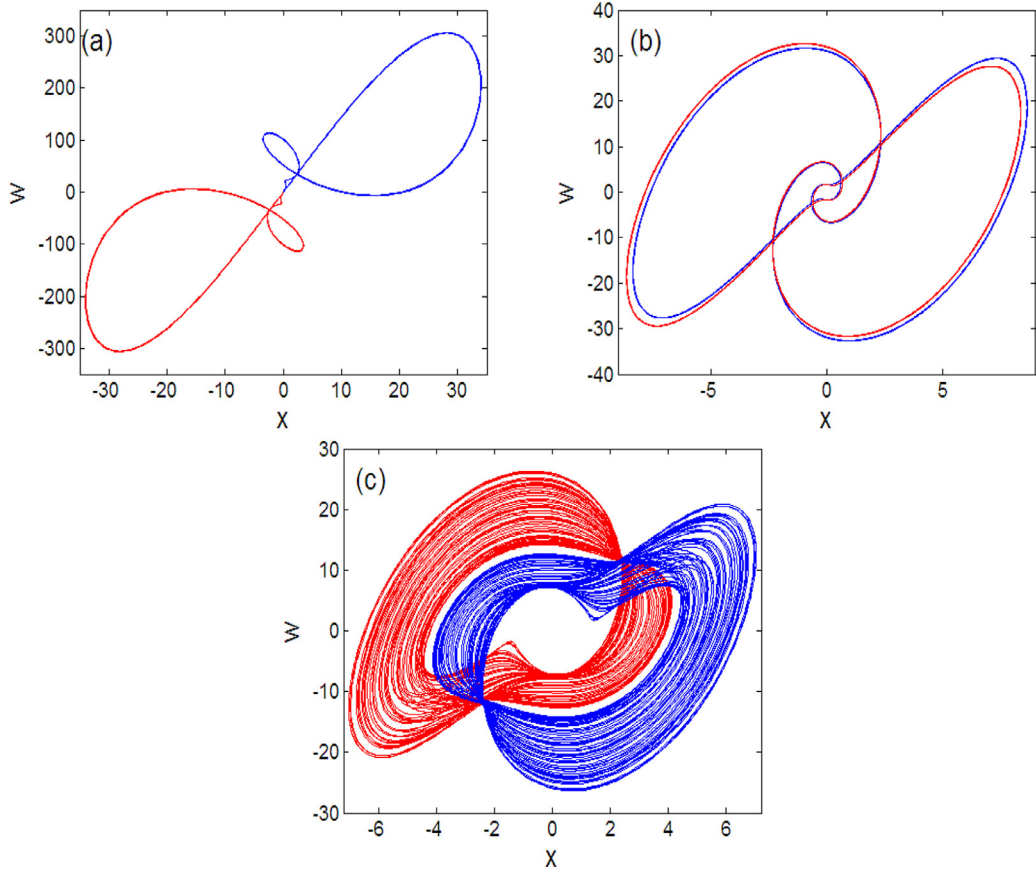


Fig. 13. Six coexisting attractors for $a = 50$, $b = 8$, $c = 10$: (a)-(b) four limit cycles with initial values $(\pm 1, 0, 0, 0)$, $(1, 1, 1, 1)$, $(1, 1, 1, -2)$; (c) two chaotic attractors with initial values $(\pm 1, \pm 1, 0, 0)$.

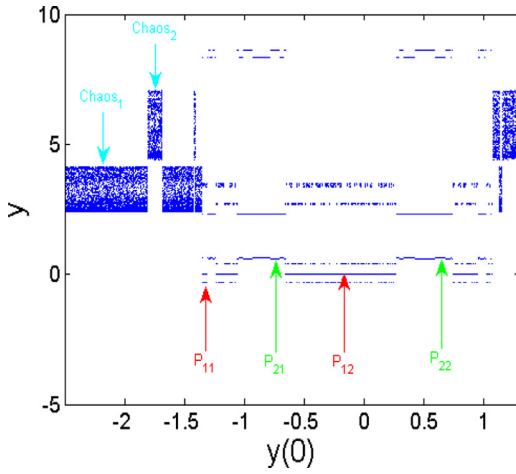


Fig. 14. Bifurcation diagram showing local maxima of the coordinate y versus initial value $y(0)$ plotted in the range $[-2.5, 1.3]$. The system parameters being fixed to $a = 50$, $b = 8$, $c = 10$ and the rest of initial values fixed as $x(0) = z(0) = w(0) = 1$.

plotting the bifurcation diagram with respect to the initial value $y(0) \in [-2.5, 1.3]$ and the fixed initial values $x(0) = z(0) = w(0) = 1$, as shown in Fig. 14.

Through the above analysis, we can conclude that system (1) emerges various types of coexisting attractors for different parameters and initial values. The bifurcation diagrams correspond to the parameters and initial values illustrate the generation and formation of the coexisting attractors in system (1). The coexistence of

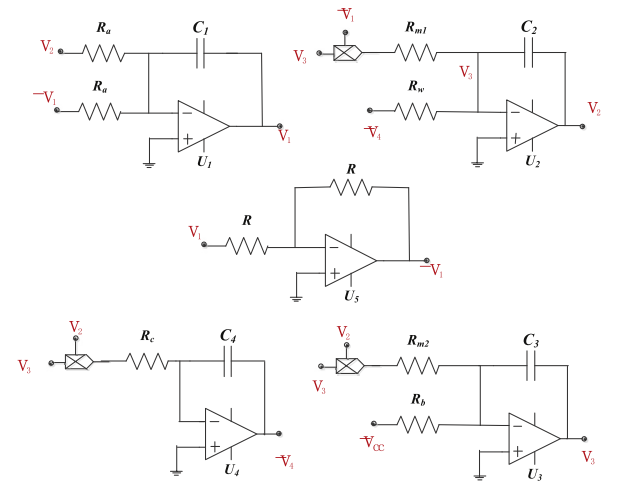


Fig. 15. Analogue electronic circuit of the system (1). The nonlinear terms are implemented by the analog multipliers (e.g. type AD633).

multiple attractors means that the system shows sensitivity to both parameters and initial values. The variation of parameters and initial values cause the dynamic evolution of the system with the occurrence of multiple bifurcation. Fix the parameters, independent bifurcations imply the generation of independent attractors with different initial values. Fix the initial values, different types of bifurcations imply different types of attractors. Generally speaking, multiple bifurcations inspired by the nonlinearity of the system

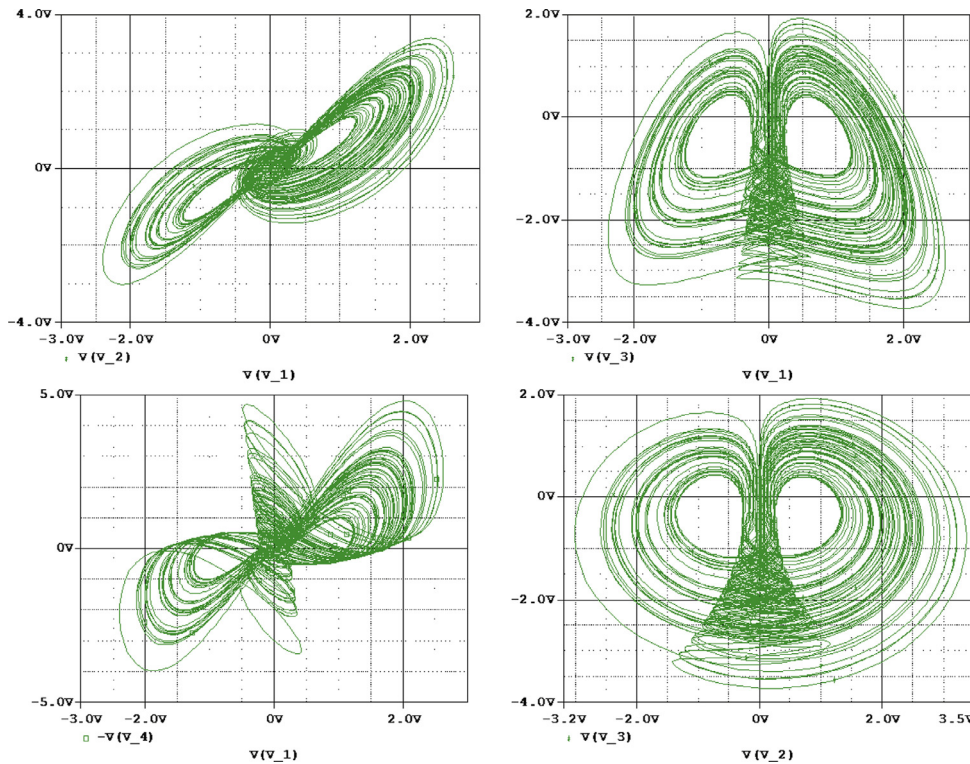


Fig. 16. Pspice simulation results in the various planes for $R_c = 1.33 \text{ k}\Omega$. The experimental initial value is $(v_1(0), v_2(0), v_3(0), v_4(0)) = (-1, -10, -10, -10)$.

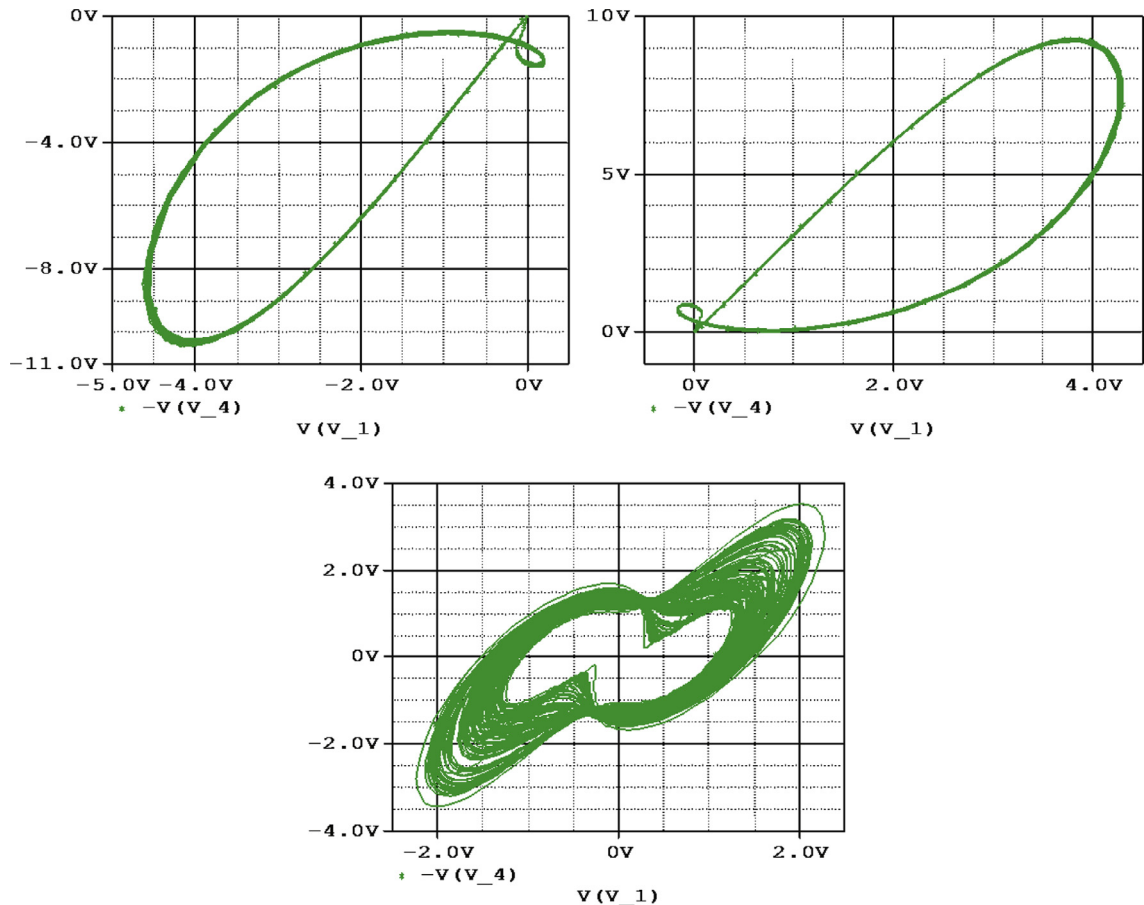


Fig. 17. Pspice simulation results showing the coexistence of three different attractors $R_a = 2 \text{ k}\Omega, R_b = 375 \text{ k}\Omega, R_c = 0.8 \text{ k}\Omega$.

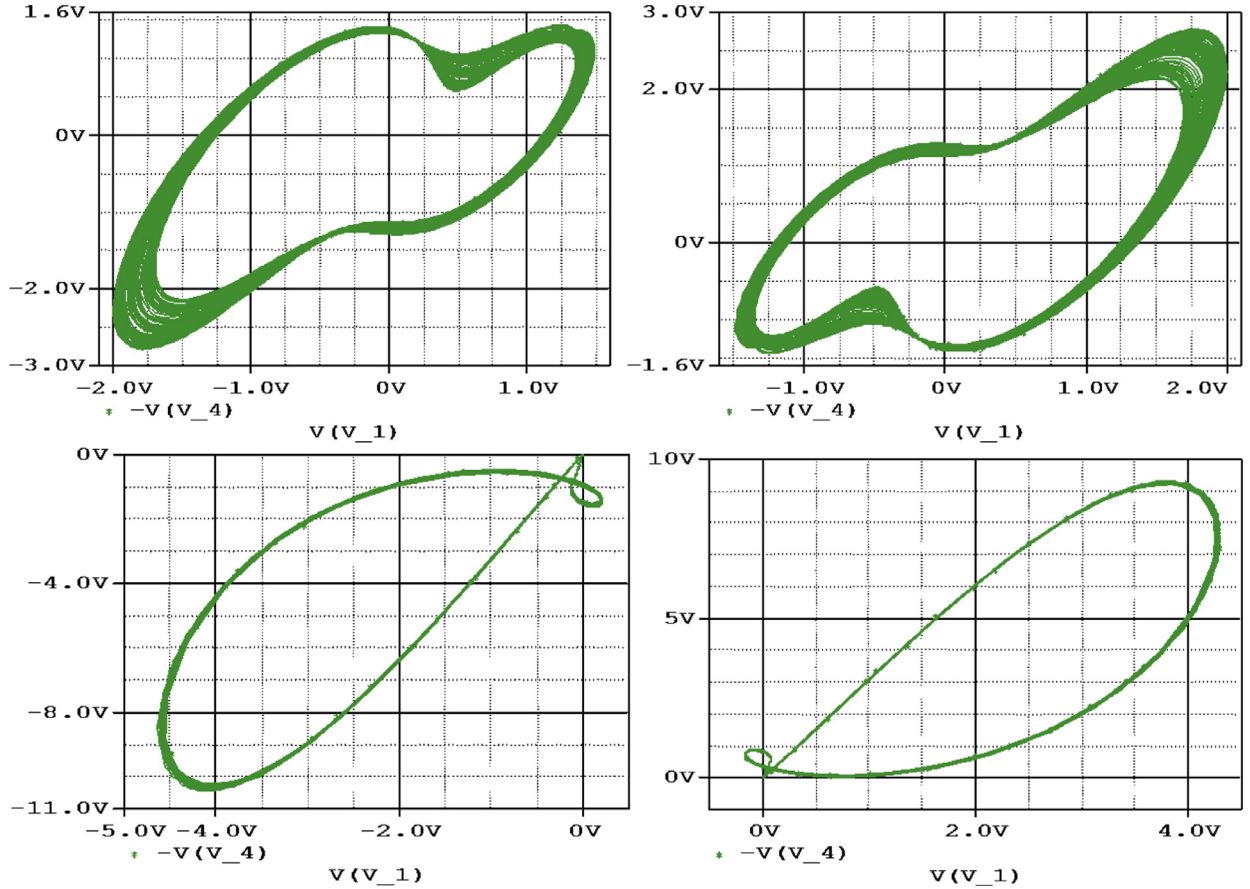


Fig. 18. Pspice simulation results showing the coexistence of four different attractors $R_a = 2 \text{ k}\Omega$, $R_b = 375 \text{ k}\Omega$, $R_c = 0.85 \text{ k}\Omega$.

itself determine the appearance of coexisting attractors to some extent.

6. Circuit implementation

The aim of this section is to design and implement an appropriate analog simulator for the analysis of the mathematical model defined in system (1). To this end, the circuit diagram of system (1) is proposed in Fig. 15. This circuit consists of four channels each implementing one of the four variables of the model. Analog devices AD633JN versions of the AD633 four-quadrant voltage multipliers chips are used to implement the nonlinear terms of the mathematical model. The operational amplifiers (type TL082 or TL084) and related circuitry implement the basic operations of subtraction, addition and integration. It is also important to rescale the model by a factor of 5 for X , Y , Z and 10 for W to avoid saturation of the output signals of operational amplifiers. The rescaled system reads

$$\begin{cases} \dot{X} = a(Y - X) \\ \dot{Y} = 2W + 5XZ \\ \dot{Z} = \frac{b}{5} - 5XY \\ \dot{W} = \frac{5cYZ}{2} \end{cases} \quad (3)$$

Upon applying the Kirchhoff's electrical circuit laws to the circuit of Fig. 15, the following set of four coupled first order differ-

ential equations can be derived

$$\begin{cases} C_1 \frac{dV_1}{dt} = \frac{(V_2 - V_1)}{R_a} \\ C_2 \frac{dV_2}{dt} = \frac{V_4}{R_b} + \frac{V_1 V_3}{10R_{m1}} \\ C_3 \frac{dV_3}{dt} = \frac{V_{cc}}{R_b} - \frac{V_1 V_2}{10R_{m2}} \\ C_4 \frac{dV_4}{dt} = \frac{V_2 V_3}{10R_c} \end{cases} \quad (4)$$

Adopting the time unit of 10-4s, the parameters of the mathematical model (1) can be expressed in terms of the circuit parameters as follows:

$$a = \frac{10^{-4}}{R_a C_1}, b = \frac{5V_{cc} 10^{-4}}{R_b C_3}, c = \frac{10^{-4}}{25R_c C_4} \quad (5)$$

The butterfly attractors are obtained by letting $R_a = 10 \text{ k}\Omega$, $R_b = 750 \text{ k}\Omega$, $R_c = 1.33 \text{ k}\Omega$ of the circuit, as shown in Fig. 16. The reverse period doubling bifurcation can also be observed with the electronic circuit simulation in Pspice using the electronic components $R_a = 10 \text{ k}\Omega$, $R_b = 750 \text{ k}\Omega$. For $R_c = 0.22 \text{ k}\Omega$, a period-1 attractor is observed. A period-2 is obtained at $R_c = 0.23 \text{ k}\Omega$. An asymmetric chaotic attractor is observed at $R_c = 2.4 \text{ k}\Omega$. For $R_c = 0.25 \text{ k}\Omega$ and $R_c = 0.4 \text{ k}\Omega$, two different symmetric chaotic attractors are obtained.

Pspice circuit simulations also confirm the coexistence of multiple attractors in the system (1) with $R_a = 2 \text{ k}\Omega$, $R_b = 375 \text{ k}\Omega$. For $R_c = 0.8 \text{ k}\Omega$, three different attractors coexist in the phase space: two periodic attractors with initial values $(v_i(0))$ given by $(-1, 0, 1, 0)$, $(1, 1, 0, 0)$ and a symmetric chaotic attractor with initial value $(v_i(0))$ given by $(1, 0, 0, 0)$ are shown

in Fig. 17. For $R_c = 0.85$ k Ω , four different attractors coexist in the phase space: two periodic attractors with initial values $(v_i(0))$ given by $(-1, 0, 1, 0), (1, 0, 0, 0)$ and two chaotic attractors with initial values $(v_i(0))$ given by $(\pm 1, \pm 1, 0, 0)$ are shown in Fig. 18.

A very good similarity between numerical phase portraits and Pspice simulation results can be observed. However, slight discrepancies that may be attributed to the simplifying assumptions adopted during the modeling process can be noted between the bifurcations points in Pspice compared to the results from the theoretical analysis.

7. Conclusions

This letter has reported the generation of a new 4D autonomous chaotic system which, very interestingly, was rich in various types of coexisting attractors. The system was yielded from the classical Sprott B system by adding an additional variable with nonlinear derivative function. It was chaotic with a butterfly attractor which can be broken into a pair of symmetric strange attractors as the parameter changes. Simulation determined the coexisting attractors of the system with different parameters and initial values, such as six periodic attractors, four periodic attractors with two chaotic attractors, two periodic attractors with three chaotic attractors, two periodic attractors with two chaotic attractors, four periodic attractors, etc. An electronic circuit was established according to the system, which confirms the dynamics of the system physically.

Acknowledgments

This work was supported by the National Natural Science Foundation of China under Grant 61603137, the Jiangxi Natural Science Foundation of China under Grant 2017BAB212016 and the Youth Science Foundation of Jiangxi Provincial Education Department under Grant GJJ150495.

References

- [1] Li CB, Sprott JC. Multistability in the Lorenz system: a broken butterfly. *Int J Bifur Chaos* 2014;24:1450131.
- [2] Leipnik RB, Newton TA. Double strange attractors in rigid body motion with linear feedback control. *Phys Lett A* 1981;86:63–76.
- [3] Leonov GA, Kuznetsov NV, Vagaitsev VI. Localization of hidden Chua's attractors. *Phys Lett A* 2011;375:2230–3.
- [4] Li CB, Sprott JC. Multistability in a butterfly flow. *Int J Bifur Chaos* 2013;23:1350199.
- [5] Sprott JC, Wang X, Chen G. Coexistence of point, periodic and strange attractors. *Int J Bifur Chaos* 2013;23:1350093.
- [6] Danca MF, Feckan M, Kuznetsov N, Chen G. Looking more closely at the Rabinovich-fabrikant system. *Int J Bifur Chaos* 2016;26:1650038.
- [7] Kengne J, Njitacke ZT, Fotsin HB. Dynamical analysis of a simple autonomous jerk system with multiple attractors. *Nonlinear Dyn* 2016;83:751–65.
- [8] Lai Q, Chen SM. Research on a new 3D autonomous chaotic system with coexisting attractors. *Optik* 2016;127:3000–4.
- [9] Zarei A. Complex dynamics in a 5-d hyper-chaotic attractor with four-wing, one equilibrium and multiple chaotic attractors. *Nonlinear Dyn* 2015;81:585–605.
- [10] Lai Q, Chen SM. Coexisting attractors generated from a new 4D smooth chaotic system. *Int J Cont Auto Syst* 2016;14:1124–31.
- [11] Wei ZC, Yu P, Zhang W, Yao M. Study of hidden attractors, multiple limit cycles from hopf bifurcation and boundedness of motion in the generalized hyperchaotic Rabinovich system. *Nonlinear Dyn* 2015;82:131–41.
- [12] Ojonyi OS, Njah AN. A 5d hyperchaotic Sprott B system with coexisting hidden attractors. *Chaos, Solit Fract* 2016;87:172–81.
- [13] Pham VT, Volos C, Jafari S, Kapitaniak T. Coexistence of hidden chaotic attractors in a novel no-equilibrium system. *Nonlinear Dyn* 2017;87:2001–10.
- [14] Shahzad M, Pham VT, Ahmad MA, Jafari S, Hadaeghi F. Synchronization and circuit design of a chaotic system with coexisting hidden attractors. *Eur Phys J Special Topics* 2015;224:1637–52.
- [15] Jafari S, Sprott JC, Nazarimehr F. Recent new examples of hidden attractors. *Eur Phys J Special Topics* 2015;224:1469–76.
- [16] Kengne J, Njitacke ZT, Kamdoum VT, Nguomkam AN. Periodicity, chaos, and multiple attractors in a memristor-based shinriki's circuit. *Chaos* 2015;25:103126.
- [17] Yuan F, Wang G, Shen Y, Wang X. Coexisting attractors in a memcapacitor-based chaotic oscillator. *Nonlinear Dyn* 2016;86:37–50.
- [18] Bao BC, Li QD, Wang N, Xu Q. Multistability in Chua's circuit with two stable node-foci. *Chaos* 2016;26:043111.
- [19] Li CB, Sprott JC, Xing H. Constructing chaotic systems with conditional symmetry. *Nonlinear Dyn* 2017;87:1351–8.
- [20] Lai Q, Chen SM. Generating multiple chaotic attractors from Sprott B system. *Int J Bifur Chaos* 2016;26:1650177.
- [21] Pisarchik AN, Feudel U. Control of multistability. *Phys Reports* 2014;540:167–218.
- [22] Angeli D, Ferrell JE, Sontag ED. Detection of multistability, bifurcations, and hysteresis in a large class of biological positive-feedback systems. *PNAS* 2004;101:1822–7.
- [23] Kondo HM, Farkas D, Denham SL, Asai T, Winkler I. Auditory multistability and neurotransmitter concentrations in the human brain. *Phil Trans R Soc B* 2016;372:20160110.
- [24] Sprott JC. Some simple chaotic flows. *Phys Rev E* 1994;50:647–50.
- [25] Jafari S, Sprott JC. Simple chaotic flows with a line equilibrium. *Chaos, Solit Fract* 2013;57:79–84.
- [26] Akgul A, Calgan H, Koyuncu I, Pehlivan I, Istanbullu A. Chaos-based engineering applications with a 3D chaotic system without equilibrium points. *Nonlinear Dyn* 2016;84:481–95.
- [27] Si GQ, Cao H, Zhang YB. A new four-dimensional hyperchaotic Lorenz system and its adaptive control. *Chin Phys B* 2011;20:010509.
- [28] Chen Y, Yang YQ. A new four-dimensional chaotic system. *Chin. Phys B* 2010;19:120510.
- [29] Lai Q, Guan ZH, Wu YH, Liu F, Zhang DX. Generation of multi-wing chaotic attractors from a Lorenz-like system. *Int J Bifur Chaos* 2013;23:1650177.
- [30] Jafari S, Pham VT, Kapitaniak T. Multiscroll chaotic sea obtained from a simple 3D system without equilibrium. *Int J Bifur Chaos* 2013;23:1650031.